Recent results and perspectives of the Monopix Depleted Monolithic Active Pixel Sensors (DMAPS)

Fabian Hügging [a],*, Marlon Barbero [b], Pierre Barrilon [b], Christian Bespin [a],
Patrick Breugnon [b], Ivan Caicedo [a], Yavuz Degerli [c], Jochen Dingfelder [a],
Tomasz Hemperek [a],[1], Toko Hirono [a],[2], Hans Krüger [a], Konstantinos Moustakas [a],[3],
Patrick Pangaud [b], Heinz Pernegger [d], Petra Riedler [d], Piotr Rymaszewski [a],[1],
Lars Schall [a], Philippe Schwemling [c], Walter Snoeys [d], Tianyang Wang [a],[4],
Norbert Wermes [a], Sinuo Zhang [a]

[a] Physikalisches Institut der Universität Bonn, Nußallee 12, Bonn, Germany
[b] CPPM, Aix Marseille University, 163 Avenue de Luminy, Marseille, France
[c] IRFU, CEA-Saclay, Batiment 141, Gif-sur-Yvette Cedex, France
[d] CERN, Espl. des Particules 1, Meyrin, Switzerland

ARTICLE INFO

ABSTRACT

The integration of readout electronics and sensors into a single entity of silicon in monolithic pixel detectors lowers the material budget while simplifying the production procedure compared to the conventional hybrid pixel detector concept. The increasing availability of high-resistivity substrates and high-voltage capabilities in commercial CMOS processes facilitates the application of depleted monolithic active pixel sensors (DMAPS) in modern particle physics experiments. TJ-Monopix2 and LF-Monopix2 chips are the most recent large-scale prototype DMAPS in their respective development line originally designed for the ATLAS Inner Tracker outer layer environment. In this contribution, the latest laboratory characterizations and beam test results of both DMAPS are presented with a special emphasis on performance after irradiation to high fluences.

1. The Monopix design

The Monopix design implements monolithic active pixel detectors in commercial CMOS imaging technologies. High-resistivity substrates with high-voltage capabilities facilitate depletion of the charge-sensitive volume, maximizing the charge collection potential and enabling fast signal generation by drift. The presented prototypes, TJ-Monopix2 and LF-Monopix2 share the same approach of having all analog and digital electronics inside the pixel unit cell. Both prototypes use the same column-drain readout architecture well known from many hybrid pixel detectors [1]. The difference between the demonstrators is the size of the charge collecting readout electrode relative to the pixel area which results into low electric field regions between pixel for the small collecting electrode design. So that the charge collection efficiency after irradiation for these designs suffers from losses in this area which are not seen in the large electrode designs.

1.1. LF-Monopix2

LF-Monopix-2 has a large collection electrode, is implemented in 150 nm LFoundry technology and features 56×340 pixels of a size of $150\,\mu m \times 50\,\mu m$. A schematic cross-section through the pixel unit cell is depicted in Fig. 1. LF-Monopix2 features a 6-bit ToT energy measurement and a 4-bit in-pixel tuning DAC. This design houses all in-pixel readout electronics inside the charge collecting readout electrode and exhibits a larger radiation tolerance by a more homogeneous electrical field w.r.t. small collecting electrode design at the cost of a higher detector capacitance of the order of 250 fF and thus a high analog power consumption of about 28 μW/pixel.
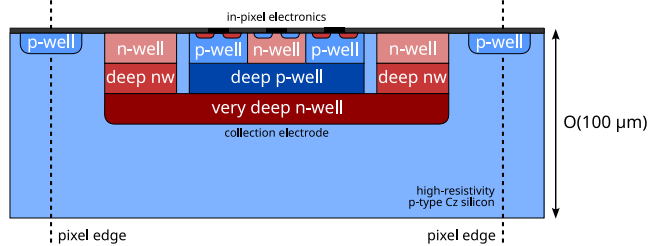

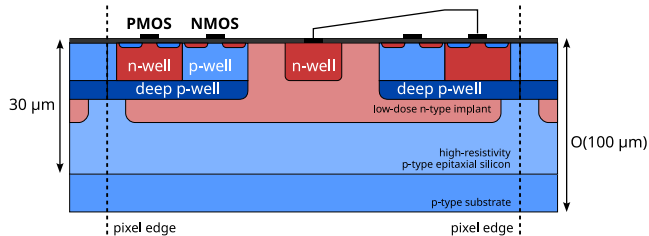**Fig. 1.** LF-Monopix2 schematic cross-section.

Fig. 2. TJ-Monopix2 schematic cross-section.

Table 1
Typical front-end performance of LF- and TJ-Monopix2 before irradiation.

	LF-Monopix2	TJ-Monopix2
Mean threshold	2000 e⁻	200 e⁻
Threshold dispersion	100 e⁻	5 e⁻
Noise (ENC)	100 e⁻	5 e⁻

1.2. TJ-Monopix2

In contrast, the TJ-Monopix2 demonstrator implemented in $180\,nm$ Tower Semiconductor technology which is based on the ALPIDE developments for ALICE [2] has a much smaller charge collection readout electrode as depicted in Fig. 2. It has 512×512 pixels of a size of $33\,\mu m \times 33\,\mu m$ and features 7-bit ToT energy measurement and a 3-bit in-pixel tuning DAC [3]. Due to the much smaller readout electrode the input detector capacitance of the TJ-Monopix2 is on in the order of only $2\,fF$ such that an excellent low analog power consumption of about $1\,\mu W/pixel$ can be achieved. To counteract the lower charge collection efficiency between pixels especially after irradiation to high fluences, a modified process has been used which features an additional low dose n-implant underneath the deep p-well which houses the in-pixel electronics [4]. In this particular design another process modification is used which features an effective gap between the low dose n-implants to further enhance charge collection between pixel [5].

2. Lab characterization

The large collection electrode of LF-Monopix2 compromises the sensors noise performance while facilitating a uniform electric field across the pixel. Therefore, LF-Monopix2 is typically operated at a threshold of $(2000 \pm 100)\,e^{-}$ with around $100\,e^{-}$ noise. Due to the small detector capacitance of TJ-Monopix2 facilitated by the small charge collection electrode, a voltage amplifier instead of a charge sensitive amplifier is the more efficient design choice for this front-end. A noise of $5\,e^{-}$ and a threshold of $(200 \pm 5)\,e^{-}$ are typical operational conditions achieved for TJ-Monopix2 after tuning. A comparison of both Monopix2 tuned front-end performances before irradiation is shown in Table 1. Since the most probable value of created charge for a traversing minimal ionizing particle differs between the two chips, both front-end responses are sufficient for a very high hit-detection efficiency [6,7].
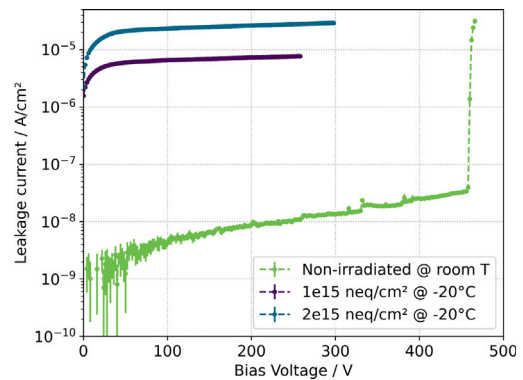

Fig. 3. IV curves of LF-Monopix2 for different fluences. At $2 \times 10^{15}\,n_{eq}\,cm^{-2}$ it is still above $300\,V$.
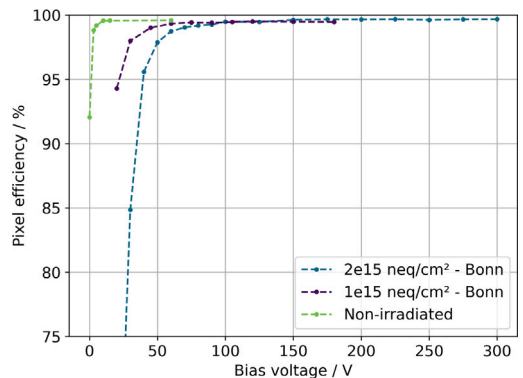

Fig. 4. Hit detection efficiency of LF-Monopix2 versus bias voltage for different fluences. No statistical errors are depicted because they are too small to be visible in this scale. A systematical error of 0.1% can be assumed. Values above 99% can be reached even for the highest fluence tested.

3. Radiation hardness

Both Monopix2 chips are designed to fulfill the ATLAS ITk outer layer requirements specifying a radiation tolerance of at least up to $1 \times 10^{15}\,n_{eq}\,cm^{-2}$ in NIEL fluence. The increased breakdown voltage of $460\,V$ measured with LF-Monopix2 before irradiation due to a an improved guard-ring structure compared to around $250\,V$ of LF-Monopix1 is shown in Fig. 3 [7,8]. For the highest available fluence of $2 \times 10^{15}\,n_{eq}\,cm^{-2}$ no breakdown was observed up to $300\,V$ which is more than sufficient to fully deplete the $100\,\mu m$ thick sensors. Fig. 4 shows the hit-detection efficiency for different bias voltages measured with LF-Monopix2 for all available proton-irradiated fluences. The >99% homogeneous efficiency measured after $2 \times 10^{15}\,n_{eq}\,cm^{-2}$ fluence at $150\,V$ biasing exceeds the specification by a factor of 2 and are a promising result for a good performance at even higher fluences.

While tests of irradiated TJ-Monopix2 are still ongoing, its predecessor TJ-Monopix1 was already intensively studied. $1 \times 10^{15}\,n_{eq}\,cm^{-2}$ neutron-irradiated TJ-Monopix1 chips have shown hit-detection efficiencies close to 99% [9]. Because of the lower threshold operation which is possible due to the 3-bit in-pixel tuning DAC, the efficiency after irradiation is expected to increase for TJ-Monopix2. Furthermore, first beam tests with proton-irradiated TJ-Monopix2 at $5 \times 10^{14}\,n_{eq}\,cm^{-2}$ fluence resulted in hit-detection efficiencies >99.9% [10].

4. Conclusion

The improved performance of LF-Monopix2 in terms of high voltage operation and hit efficiency after higher fluences facilitates its high radiation hardness which exceeds the design specification and the

performance of its predecessor by at least a factor of 2. Encouraged by the very good hit-detection efficiency >99% after proton-irradiation up to 2×10^{15} n_{eq} cm^{-2}, the sensor will be tested at even higher fluences. The optimized front-end of TJ-Monopix2 provides lower operational thresholds compared to its predecessor. This improvement is expected to result in an excellent hit-detection efficiency at irradiation levels of 1×10^{15} n_{eq} cm^{-2} and higher. First beam test results of proton-irradiated sensors to 5×10^{14} n_{eq} cm^{-2} support this expectation.

Declaration of competing interest

The authors declare that they have no known competing financial interests or personal relationships that could have appeared to influence the work reported in this paper.

Acknowledgments

References

[1] I. Peric, et al., The FEI3 readout chip for the ATLAS pixel detector, Nucl. Instrum. Methods A 565 (2006) 178–187, http://dx.doi.org/10.1016/j.nima.2006.05.032.

[2] M. Mager, (ALICE), ALPIDE, the monolithic active pixel sensor for the ALICE ITS upgrade, Nucl. Instrum. Methods A 824 (2016) 434–438, http://dx.doi.org/10.1016/j.nima.2015.09.057.

[3] K. Moustakas, Design and Development of Depleted Monolithic Active Pixel Sensors with Small Collection Electrode for High-Radiation Applications (Ph.D. thesis), Rheinische Friedrich-Wilhelms-Universität Bonn, 2021, URL: https://hdl.handle.net/20.500.11811/9315.

[4] W. Snoeys, et al., A process modification for CMOS monolithic active pixel sensors for enhanced depletion, timing performance and radiation tolerance, Nucl. Instrum. Methods A 871 (2017) http://dx.doi.org/10.1016/j.nima.2017.07.046.

[5] M. Muenker, Simulations of CMOS pixel sensors with a small collection electrode, improved for a faster charge collection and increased radiation tolerance, J. Instrum. 14 (05) (2019-05) http://dx.doi.org/10.1088/1748-0221/14/05/C05013.

[6] C. Bespin, et al., Charge collection and efficiency measurements of the TJ-Monopix2 DMAPS in 180 nm CMOS technology, PoS Pixel2022 (2023) 080, http://dx.doi.org/10.22323/1.420.0080.

[7] I. Caicedo, et al., Improvement in the design and performance of the Monopix2 reticle-scale DMAPS, in: JPS Conf. Proc., Vol. VERTEX2022, 2024, http://dx.doi.org/10.7566/JPSCP.42.011021.

[8] L. Schall, et al., Test-beam performance of proton-irradiated, large-scale depleted monolithic active pixel sensors in 150 nm CMOS technology, PoS VERTEX2023 (2024) 043, http://dx.doi.org/10.22323/1.448.0043.

[9] C. Bespin, et al., Development and characterization of a DMAPS chip in TowerJazz 180 nm technology for high radiation environments, Nucl. Instrum. Methods A 1040 (2022) http://dx.doi.org/10.1016/j.nima.2022.167189.

[10] M. Babeluk, et al., The DMAPS upgrade of the Belle II vertex detector, Nucl. Instrum. Methods A 1064 (2024) http://dx.doi.org/10.1016/j.nima.2024.169428.